Optical Properties of ZnO Nanoparticles Synthesised from a Polysaccharide and $ZnCl_2$

P. Bindu[a,b,*] and S. Thomas[a,b]

[a]School of Chemical Sciences, Mahatma Gandhi University,
Priyadarshini Hills P.O, Kottayam, Kerala, India 686 560

[b]International and Inter University Centre for Nanoscience and Nanotechnology, Mahatma Gandhi University,
Kottayam, Kerala, India 686 560

(Received March 28, 2016; in final form March 17, 2017)

In this article we study the optical properties of ZnO nanoparticles. This paper describes cost effective, high yield, and a facile synthetic method for the synthesis of ZnO nanoparticles from precursors viz. linear polysaccharide, chitosan, and $ZnCl_2$ by a precipitation method. The synthesized ZnO nanoparticles were characterized by surface area, pore size, and UV-visible measurements. The optical band gap and the Urbach energy were also calculated and the optical band gap energy of the synthesized ZnO nanoparticles was found to be 3.26 eV and the nature of the optical transition has been identified as direct allowed.

DOI: 10.12693/APhysPolA.131.1474

PACS/topics: ZnO nanoparticles, UV-vis, band gap, Urbach energy

1. Introduction

Recently, ZnO nanoparticles have attracted great potential interest compared to TiO_2 nanoparticles [1], due to its highly versatile and promising applications in varistors, electrostatic dissipative coating, catalysts for liquid phase hydrogenation and photo-catalytic degradation, gas sensors, electrical and optical devices, chemical absorbent and solar cells. It has also attracted attention as a promising phosphor for field emission displays (FEDs) [2] compared with the conventional sulfide phosphors. The biggest users of ZnO are manufacturers of rubber; the content of ZnO in vulcanized rubber can be reduced to 10 times if nanosized ZnO is used instead of the conventional micro ZnO [3]. Previous research reports [4–6] revealed that the vulcanized rubber products can last longer and have improved properties if nanosized ZnO is used as the activator and accelerator instead of micro ZnO, and this approach in turn can greatly reduce the quantity of micro ZnO in the vulcanization of rubber [5, 6] and the release of toxic zinc metal into the environment [6].

Size controlled inorganic nanoparticles viz. metals, semiconductors, and metal oxides have attracted great interests because of their material properties compared with their bulk. Hence, investigations on the synthesis and modification of ZnO nanoparticles have attracted tremendous attention. Owing to the high surface to volume ratio of ZnO nanostructures, the nature of the surface is very important when considering the properties of ZnO nanoparticles. Many methods for the synthesis of ZnO nanoparticles have been reported [7], viz. microemulsion synthesis, sol gel technique, mechanochemical processing, spray pyrolysis and drying, thermal decomposition of organic precursor, RF plasma synthesis, supercritical-water processing, self assembling, hydrothermal processing, vapour transport process, sonochemical or microwave assisted synthesis, direct precipitation, and homogeneous precipitation.

In this work, we investigate the optical properties of ZnO nanoparticles synthesized from chitosan and $ZnCl_2$. The optical band gap and the Urbach energy were also calculated and reported. The surface area and average pore size of the synthesised ZnO nanoparticles were determined and reported. We have found that this is a cost effective and facile method for the synthesis of ZnO nanoparticles. The structure and morphology of ZnO nanoparticles were investigated by the Fourier transform infrared (FTIR), X-ray diffraction (XRD), scanning electron microscopy (SEM), transmission electron microscopy (TEM) and photoluminescence (PL) studies and reported in our previous paper [6]. ZnO has wide range of applications in various fields. Hence scaling up of the process towards synthesis of ZnO nanoparticles with high purity and excellent yield seems efficient.

2. Experimental

2.1. Materials

Chitosan was provided by M/s. India Sea Foods, Cochin, Kerala, India. Zinc chloride and sodium hydroxide were supplied by M/s. S. D. Fine Chem. Ltd., Mumbai, India. ZnO nanoparticles were synthesized from Chitosan, zinc chloride, and sodium hydroxide.

2.2. Sample preparation. Synthesis of ZnO nanoparticles

ZnO nanoparticles were synthesized from zinc chloride and chitosan [4, 8]. In the present synthetic procedure

*corresponding author; e-mail: bindu_patanair@yahoo.com

we have modified the reaction conditions to facilitate the formation of Zn–chitosan complex and also try to increase the yield of the ZnO nanoparticles. We have modified the concentrations of $ZnCl_2$, chitosan and NaOH, pH of the reaction medium, reaction temperature and stirring time for complexation of Zn–chitosan complex and precipitation of $Zn(OH)_2$ out of the complex. $ZnCl_2$ (5 g) was dissolved in 100 ml 1% acetic acid to form 5% solution. Another 1% solution of chitosan was prepared in 1% acetic acid. Both the solutions were mixed (pH 5.5–6) and stirred at 45 °C for 21 h. After this, stoichiometric amount of NaOH (5%) was added drop wise to the above mixture (pH 10) with constant stirring. The whole mixture was then allowed to digest for 24 h at room temperature. During this time OH^- and Cl^- ions were diffused through the medium and white gel like precipitate of $Zn(OH)_2$ was formed. This was filtered and washed thoroughly with distilled water to remove un-reacted Chitosan and other by product like NaCl. This was then dried at 100 °C and calcined at 550 °C for 4 h in a muffle furnace to get ZnO nanocrystals. The yield of ZnO nanocrystals obtained by this method is about 90%. This facile synthetic route has the following advantages: the reaction can be carried out under moderate conditions, yield of the product is very good and particles of nanometer size can be attained, which makes this method promising for large scale production. A schematic representation of the synthetic route is given below.

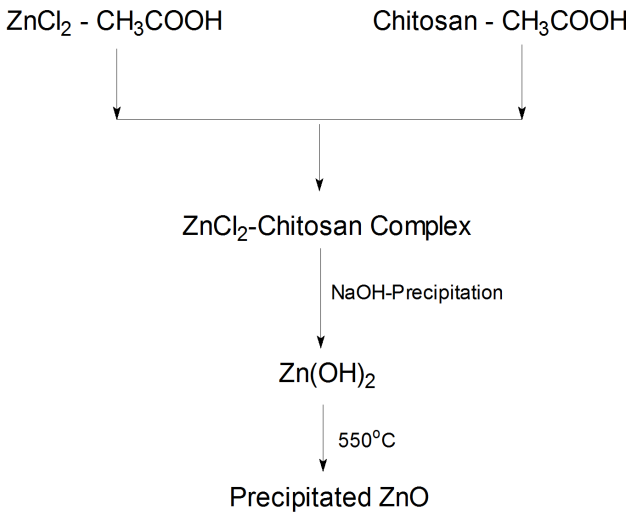

The chitosan is a linear polymine with reactive anino groups and hydroxyl groups available and hence can easily form chelates with transition metal ions. $–NH_2$, –OH and –NHCO– (–NHCO– in deacetylated form) of chitosan molecule were coordinated to Zn(II). The $–NH_2$, –OH groups in chitosan molecule were considered as the dominating reactive sites. In the present reaction chitosan acts as a chelating agent for Zn^{2+} ions to form Zn–chitosan complex.

2.3. Characterization

The surface area of ZnO nanoparticles was determined by using Micromeritics-ASAP 2020 Surface Area and Porosity Analyser (Software V3.01G). The optical absorption spectrum was recorded with UV-2400PC, in the wavelength range 250–850 nm.

3. Results and discussion

The synthesized ZnO nanoparticles were characterized by FTIR, XRD, SEM, TEM, and PL spectrum [6]. The XRD pattern of synthesised ZnO nanoparticles was explained in our previous report [6]. The broadening of peak in the XRD pattern clearly implies that small nanocrystals are present in the samples. There is no evidence of bulk remnant materials and impurity. In the XRD pattern, the {101} diffraction peak is much stronger than {002} peak. This indicates that the formed ZnO nanocrystals have a preferential crystallographic {101} orientation [6].

The surface area of ZnO nanoparticles measured by the Brunauer–Emmett–Teller (BET) method was found to be 36.56 m^2/g and average pore diameter was 25.35 nm. The surface area of nanoparticles varies with the reaction conditions and the various synthetic routes adopted. We have made a correlation of the synthetic route explained by other researchers [4, 8, 9] using chitosan as one of the precursors for the preparation of ZnO nanoparticles and the properties of ZnO nanoparticles were presented in Table I.

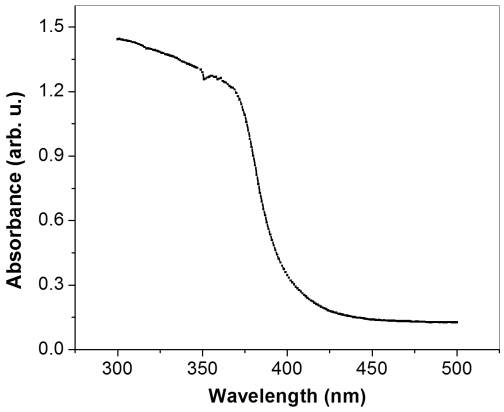

Fig. 1. UV-vis absorption spectrum of ZnO nanoparticles.

The optical absorbance spectrum of synthesized ZnO nanoparticles was shown in Fig. 1. The UV-visible spectrum displayed the excitonic absorption peak at 360 nm which implies the lower particle size of ZnO and the absorption peak lies much below the band gap wavelength of 388 nm of bulk ZnO [10]. The weak absorption area covers almost the whole of the visible field ranging between 400 nm and 800 nm. In the modified synthetic route, the surface area and absorption peak of ZnO nanoparticles are little smaller than that of Ref. [4], however,

TABLE I

The correlation of different synthetic routes adopted for the preparation of ZnO nanoparticles with its properties.

Precursor used	Stirring time	NaOH added	Surface area ZnO nano-particles [m^2/g]	Crystallite size XRD [nm]	Particle size TEM [nm]	Average pore diameter [nm]	Absorption peak [nm]	Refs.
5:1 $ZnCl_2$: chitosan, in acetic acid, (pH 5.5–6)	21 h at 45 °C, continuous moderate stirring	5%, pH 10, 24 h at RT, continuous moderate stirring	36.56	27.49	20–50	25.35	360	present work and [6]
1:2 $ZnCl_2$: chitosan, in acetic acid	24 h at RT, continuous vigorous stirring	12 h at RT, continuous stirring	42.15	18.78	12–30	–	368	[4]
1:1 $ZnCl_2$: chitosan, in acetic acid	24 h at RT, continuous vigorous stirring	5% in 1% acetic acid, 12 h at RT, continuous stirring	–	13.4	45–60	–	–	[8]
1:1 $Zn(NO_3)_2$: chitosan in deionized distilled water	6 h at RT, continuous stirring	–	23.77	–	31–42	9.70	–	[9]
1:1 $Zn(NO_3)_2$: modified chitosan, in deionized distilled water	6 h at RT, continuous stirring	–	15.45	–	19–54	221.40	–	[9]

crystallite size calculated from XRD (by using Debye–Scherrer's equation) and particle size from TEM are higher than that reported in Ref. [4]. The pore size is higher than that reported in Ref. [9] for unmodified chitosan as the precursor. Table I reveals that surface area and particle size depend on the proportion of precursors, pH of the reaction medium, stirring time and speed, concentration of added NaOH and its pH. In order to evaluate the threshold wavelength (λ_s) value, UV-vis spectrum has been analysed according to the following equation [11],

$$(A/\lambda)^2 = K(1/\lambda - 1/\lambda_s), \tag{1}$$

where A, λ, and K are absorbance, wavelength, and an empirical constant, respectively. Plotting $(A/\lambda)^2$ vs. $1/\lambda$ from spectrum, the λ_s value was obtained from the intersection of the tangent drawn to the inflection point with the baseline (Fig. 2). The calculated value of threshold wavelength λ_s was found to be 376 nm.

The absorption coefficient α associated with the strong absorption region of the sample was calculated from absorbance A and the sample thickness t. It was calculated by the relation [12]:

$$\alpha = 2.3026A/t. \tag{2}$$

The optical band gap can be estimated using the following Tauc relation [13]:

$$\alpha h\nu = B(h\nu - E_g)^n, \tag{3}$$

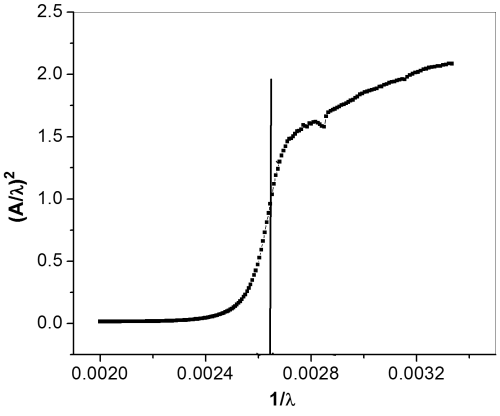

Fig. 2. Plot of $(A/\lambda)^2$ vs. $1/\lambda$ of ZnO nanoparticles.

where B is a constant and E_g is the optical band gap of the material, n is a number which characterizes the nature of electronic transition between valance band and

conduction band, which may have values 1/2, 2, 3/2, and 3 corresponding to the allowed direct, allowed indirect, forbidden direct, and forbidden indirect transitions, respectively. It is well known that direct transition across the band gap is feasible between the valence and the conduction band edges in "k space". In the transition process, the total energy and momentum of the electron–photon system must be conserved. It is known that ZnO is a direct band gap semiconductor, then from the above equation, it is clear that plot of $(\alpha h\nu)^2$ vs. $h\nu$ will indicate a divergence at an energy value E_g, where the transition takes place. The band gap value depends on the nature of the transition (i.e., the n value) determined.

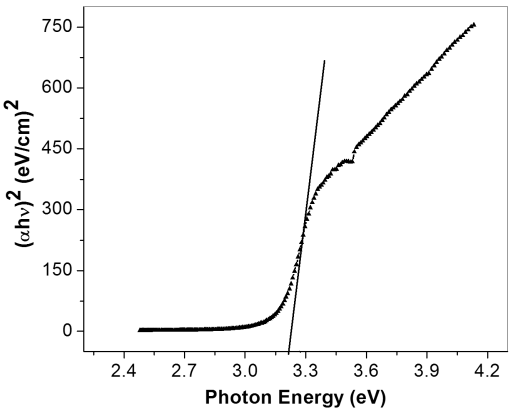

Fig. 3. Plot of $(\alpha h\nu)^2$ vs. $h\nu$ of ZnO nanoparticles.

The estimated band gap from the plot of $(\alpha h\nu)^2$ vs. $h\nu$ for ZnO nanoparticles can be seen in Fig. 3. The band gap "E_g" is determined by extrapolating the straight portion to the energy axis at $\alpha = 0$. The linear part shows that the mode of transition in these nanoparticles is direct in nature. The estimated band gap value of the ZnO nanoparticle was found to be 3.26 eV. The band gap value is less than that of bulk ZnO 3.37 eV, this might be due to the strain arising from chemical synthesis of ZnO nanoparticle. These micro-strains highly influence the optical band gap of material [14].

For allowed indirect transitions the value of $n = 2$ in the Tauc relation and plot of $(\alpha h\nu)^{1/2}$ vs. $h\nu$ for ZnO nanoparticles was given in Fig. 4. By extrapolating the straight portion to the energy axis at $\alpha = 0$, the band gap "E_g" can be estimated and it was found to be 3.0 eV. Since the band gap energy is higher for direct allowed transition, it was confirmed that the mode of transition in these ZnO nanoparticles is direct in nature.

It is also assumed that the absorption coefficient near the band edge shows an exponential dependence on photon energy and this dependence is given as follows [15, 16]:

$$\alpha = \alpha_0 \exp(h\nu/E_u), \tag{4}$$

where α_0 is a constant and E_u is the Urbach energy interpreted as the width of the tails of localized states, associated with the amorphous state, in the forbidden gap. The plot of $\ln\alpha$ vs. photon energy is shown in Fig. 5.

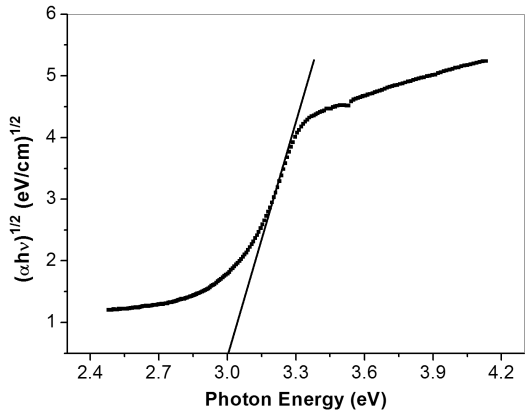

Fig. 4. Plot of $(\alpha h\nu)^{1/2}$ vs. $h\nu$ of ZnO nanoparticles.

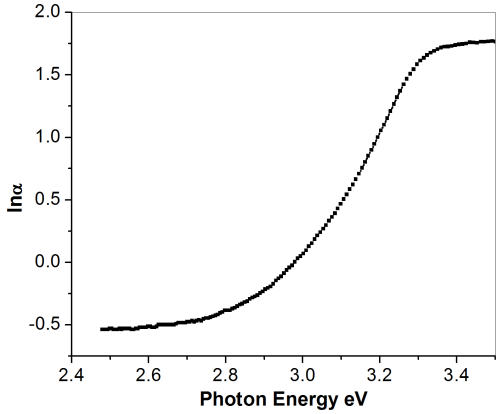

Fig. 5. Plot of $\ln\alpha$ vs. $h\nu$ of ZnO nanoparticles.

The value of E_u is calculated by taking the reciprocal of the slopes of the linear portion in the lower photon energy region of the curve and the value of the Urbach energy was found to be 489.78 meV (0.49 eV). It is believed that the exponential dependence of photon energy may arise from random fluctuations of the internal fields associated with the structural disorder in many crystalline and amorphous materials. This is probably due to the structural disorders in the sample, which leads to an extension of the parabolic density of states into the band edge. These defects are originating during the crystal growth process, causing lattice disorders and generating stress in the sample. Materials with larger Urbach energy would have greater tendency to convert weak bonds into defects. The Urbach energy E_u is very important tool to investigate structural disorder in thin films [17].

4. Conclusions

The properties of ZnO nanoparticles synthesized from chitosan and $ZnCl_2$ by a modified procedure have been summarised. The optical properties of the prepared ZnO nanoparticles have been studied. The UV-visible spectrum showed the excitonic absorption peak at 360 nm, which implies the lower particle size of ZnO. This value is less than that reported in [4]. The optical band gap energy is found to be 3.26 eV and the optical

transition is direct allowed. The Urbach energy was calculated and found to be 489.78 meV (0.49 eV). The surface area and average pore diameter is 36.56 m^2/g and 25.35 nm, respectively. The modified synthetic method favoured the higher pore diameter and lower absorption peak of ZnO nanoparticles.

Acknowledgments

One of the authors, P. Bindu thanks the Department of Science and Technology (DST), New Delhi, India, for the award of Young Scientist Fellowship and financial assistance for carrying out the research project. Thanks to Prof. Subhadra Patanair, Former Head, Department of Mathematics, S.N.M. College Maliankara, Ernakulam, India and Prof. Dr. C. Jacob, Materials Science Centre, Indian Institute of Technology (IIT), Kharagpur, India for valuable suggestions and help.

References

[1] G.P. Fotou, S.E. Pratsinis, *Chem. Eng. Commun.* **151**, 251 (1996).

[2] Z. Zhang, H. Yuan, J. Zhou, D. Liu, S. Luo, Y. Miao, Y. Gao, J. Wang, L. Liu, L. Song, Y. Xiang, X. Zhao, W. Zhou, S. Xie, *J. Phys. Chem. B* **110**, 8566 (2006).

[3] G. Heideman, R.N. Datta, J.W.M. Noordermeer, B. van Baarle, *J. Appl. Polym. Sci.* **95**, 1388 (2005).

[4] K.V. Aswathy, R. Joseph, *Int. J. Plastics Technol.* **12**, 957 (2008).

[5] P.M.S. Begum, R. Joseph, K.K.M. Yusuff, *Prog. Rubber Plast. Recycling Tech.* **24**, 141 (2008).

[6] P. Bindu, S. Thomas, *J. Theor. Appl. Phys.* **8**, 123 (2014).

[7] M.S. Niasari, F. Davar, M. Mazaheri, *Mater. Lett.* **62**, 1890 (2008).

[8] K.E. Saisy, S.M. Kumar, K. Priyanka, R. Joseph, *J. Polym. Mater.* **30**, 79 (2013).

[9] M. Thirumavalavan, Kai-Lin Huang, J.F. Lee, *Materials* **6**, 4198 (2013).

[10] P. Kumbhakar, D. Singh, C.S. Tiwary, A.K. Mitra, *Chalcogenide Lett.* **5**, 387 (2008).

[11] E. Caponetti, L. Pedone, D. Chillura Martino, V. Panto, V. Turco Liveri, *Mater. Sci. Eng.* **23**, 531 (2003).

[12] M. Srivastava, A.K. Ojha, S. Chaubey, A. Materny, *J. Alloys Comp.* **481**, 515 (2009).

[13] S. Maensiri, C. Masingboon, V. Promarak, S. Seraphin, *Opt. Mater.* **29**, 1700 (2007).

[14] V. Srikanth, D.R. Clarke, *J. Appl. Phys.* **81**, 6357 (1997).

[15] F. Urbach, *Phys. Rev.* **92**, 1324 (1953).

[16] F. Yakuphanoglu, M. Sekerci, *Opt. Appl.* **2**, 209 (2005).

[17] M. Caglar, S. Ilican, Y. Caglar, *Thin Solid Films* **517**, 5023 (2009).